





# Shroom3, a Gene Associated with CKD, Modulates Epithelial Recovery after AKI

Aihua Li,<sup>1</sup> Joanna Cunanan <sup>1</sup>, Hadiseh Khalili,<sup>1</sup> Timothy Plageman <sup>2</sup>, Kjetil Ask <sup>3</sup>, Ahsan Khan,<sup>1</sup> Ashmeet Hunjan,<sup>1</sup> Thomas Drysdale,<sup>4</sup> and Darren Bridgewater <sup>1</sup>

## Key Points

- The fundamental science behind the genetic associations of Shroom3 with CKD is a knowledge gap in molecular nephrology.
- Shroom3 regulates actomyosin dynamics in kidney tubular epithelium after AKI.
- This study supports that Shroom3 is a molecular player in tubular repair and provides insight into the genetic associations of Shroom3 and CKD.

## Abstract

**Background** Ischemia-induced AKI resulting in tubular damage can often progress to CKD and is a common cause of nephrology consultation. After renal tubular epithelial damage, molecular and cellular mechanisms are activated to repair and regenerate the damaged epithelium. If these mechanisms are impaired, AKI can progress to CKD. Even in patients whose kidney function returns to normal baseline are more likely to develop CKD. Genome-wide association studies have provided robust evidence that genetic variants in Shroom3, which encodes an actin-associated protein, are associated with CKD and poor outcomes in transplanted kidneys. Here, we sought to further understand the associations of Shroom3 in CKD.

**Methods** Kidney ischemia was induced in wild-type (WT) and *Shroom3* heterozygous null mice (*Shroom3*<sup>Gt/+</sup>) and the mechanisms of cellular recovery and repair were examined.

**Results** A 28-minute bilateral ischemia in *Shroom3*<sup>Gt/+</sup> mice resulted in 100% mortality within 24 hours. After 22-minute ischemic injury, *Shroom3*<sup>Gt/+</sup> mice had a 16% increased mortality, worsened kidney function, and significantly worse histopathology, apoptosis, proliferation, inflammation, and fibrosis after injury. The cortical tubular damage in *Shroom3*<sup>Gt/+</sup> was associated with disrupted epithelial redifferentiation, disrupted Rho-kinase/myosin signaling, and disorganized apical F-actin. Analysis of MDCK cells showed the levels of Shroom3 are directly correlated to apical organization of actin and actomyosin regulators.

**Conclusion** These findings establish that Shroom3 is required for epithelial repair and redifferentiation through the organization of actomyosin regulators, and could explain why genetic variants in Shroom3 are associated with CKD and allograft rejection.

KIDNEY360 3: 51–62, 2022. doi: <https://doi.org/10.34067/KID.0003802021>

## Introduction

The kidney has evolved tubular reparative mechanisms after AKI that facilitate complete recovery and re-establishment of kidney function (1). This involves poorly functioning or damaged tubular cells being removed by cell death (2), and the remaining undamaged epithelium undergoing dedifferentiation to mesenchymal cells (3). The dedifferentiated epithelial cells then proliferate, undergoing cell migration and changes in cell shape (4). This results in the integration of the newly formed tubular epithelial cells, which repair the damaged tubular regions. Although

many patients make a full functional recovery, an AKI is associated with increased incidents of CKD, ESKD, and mortality (5,6). Although the mechanisms of recovery after AKI are multifactorial, maladaptive or incomplete epithelial repair at the subcellular level is a major contributing factor (7).

Large-scale genome-wide association studies have consistently identified numerous genetic variants in *SHROOM3* as being highly associated with CKD (8,9), reduced eGFR (9), increased albumin-creatinine ratio (10), and low serum magnesium levels (11). Furthermore, donor kidneys with genomic variants in

<sup>1</sup>Department of Pathology and Molecular Medicine, McMaster University, Hamilton, Canada

<sup>2</sup>College of Optometry, The Ohio State University, Columbus, Ohio

<sup>3</sup>Department of Medicine, McMaster University, Hamilton, Canada

<sup>4</sup>Department of Physiology and Pharmacology, University of Western Ontario, London, Canada

**Correspondence:** Dr. Darren J. Bridgewater, McMaster University, Department of Pathology and Molecular Medicine, Health Sciences Centre, 1280 Main Street West, Hamilton, Ontario, Canada. Email: [bridgew@mcmaster.ca](mailto:bridgew@mcmaster.ca)

*SHROOM3* transplanted into a recipient are associated with chronic allograft rejection, characterized by reduced eGFR, increased fibrosis, and nephropathy (12). Shroom3 is an actin-binding protein that facilitates the subcellular localization of actin to the apical region of epithelial cells (13–15). Subsequently, the recruitment and interaction of Shroom3 with Rho-kinase (ROCK) and downstream activation of nonmuscle myosin II results in the contraction of actomyosin, leading to cell shape changes and tissue morphogenesis (16). These Shroom3-regulated morphologic processes are essential for epithelial morphogenesis during the development of several organs, including the neural tube (17), lens (18), gut (19), thyroid (20), heart (21), and kidney (22). During embryonic kidney development, Shroom3 homozygous null mice exhibit several abnormally forming nephrons early in kidney development, which leads to a reduced glomerular number at birth (22). Although Shroom3 homozygous null mice are embryonically lethal due to exencephaly (23), the postnatal analysis of 1-year-old Shroom3 heterozygous null mice exhibit podocyte foot process effacement and kidney disease, resulting from disrupted ROCK/nonmuscle myosin II signaling, which disrupts actin dynamics (22). Several other studies analyzing *Shroom3* genomic variants also demonstrated podocyte cytoskeletal abnormalities leading to albuminuria and CKD (24–26). Altogether, these studies confirm essential roles for Shroom3 in kidney development and maintenance of kidney function.

The remarkable reparative processes of the kidney, from initial injury to repair and cell migration, are dependent on the modulation of the actin cytoskeleton (27). Yet, the molecules and pathways that modulate the actin dynamics during kidney injury and repair are not well understood. Given Shroom3 is associated with CKD, transplant rejection, and reduced kidney function, we hypothesize that Shroom3 may be a contributing factor in recovery and repair after a kidney injury, and investigated this possibility in this manuscript.

## Materials and Methods

### Mice Procedures

Shroom3 heterozygous mutant mice were originally generated by Hildebrand and Soriano (1999) by the insertion of a gene-trap (Gt) SA $\beta$ galCrepA cassette between exons 3 and 4 of the *Shroom3* gene. The insertion blocks splicing from exon 3 and 4 and creates a fusion RNA encoding beta-galactosidase and cre recombinase (23). Because of the gene-trap insertion, there is no detectable mRNA encoded by exon 4 and onwards. These mice are therefore termed Shroom3<sup>Gt/+</sup> (Gt) and the other allele is Wild-type (WT), (+ for WT). Genotyping was performed as previously described (22). Shroom3<sup>Gt/+</sup> were bred to WT CD1 mice and WT littermates were used as controls. All animal studies were performed in accordance with animal care guidelines set by the Animal Research Ethics Board at McMaster University (Animal Utilization Protocol #18–03–12). Ischemia/reperfusion (I/R) surgical procedures were performed on 3-month-old Shroom3<sup>Gt/+</sup> heterozygous and wild type as described for 28 and 22 minutes (48). Sham-operated control mice did not receive the ischemia/reperfusion. Kidney function was assayed by serum creatinine assay kit (Sigma

Aldrich, St. Louis, MO, USA) using retro-orbital blood samples at 0 hours (baseline, before ischemia reperfusion kidney injury [IRI]), 24 hours, 48 hours, 3 days, 5 days, 7 days, and 10 days after ischemia/reperfusion.

### Histology and Immunologic Techniques

Kidneys were resected 48 hours and 10 days after ischemia/reperfusion, and fixed in 4% paraformaldehyde for 24 hours, processed for histology, and stained with H&E, PAS, and PSR (Sigma Aldrich, Oakville, ON, Canada). Immunohistochemistry (IHC) and immunofluorescence was performed as described (41). For mouse monoclonal primary antibodies, mouse-on-mouse blocking reagents (Vector Laboratories, Burlingame, CA, USA) were used, per manufacturer protocols. Primary antibodies used were Shroom3 (gift from Dr. Timothy Plageman, Ohio State University),  $\alpha$ SMA-IF (Sigma Aldrich, 1:100), F4/80 (Santa Cruz Biotechnology, 1:200),  $\alpha$ SMA-IHC (Agilent (Dako), 1:100), PDGFR $\beta$  (Cell Signaling Technology, 1:100), CD206 (Abcam, 1:1500), Caspase-3 (Invitrogen, 1:200), Vimentin (Santa Cruz Biotechnology, 1:200), neural cell adhesion molecule (NCAM) (Sigma Aldrich, 1:100), Ki-67 (Abcam, 1:200), N-cadherin (Santa Cruz Biotechnology, 1:100), E-cadherin (Abcam, 1:100), beta-catenin (BD Biosciences, 1:200), kidney injury molecule 1 (Kim1; Novus Biologicals, 1:100), F-actin (Bioss Antibodies, 1:200), and phosphomyosin light chain (Cell Signaling Technology, 1:200). Secondary antibodies used were biotinylated anti-mouse or anti-rabbit (Vector Laboratories, 1:200), anti-mouse Dylight 594 (Thermo Fisher Scientific, 1:1000), and anti-rabbit AlexaFluor 488 (Thermo Fisher Scientific, 1:1000). All images were captured using the CellSens acquisition software (Olympus Life Science, Waltham, MA, USA) from the Olympus BX80 light and fluorescence microscope.

### Quantification of Fibrosis, F4/80, Apoptosis, Proliferation, and Kim1

In total, 10 randomly selected fields from six WT and six Shroom3<sup>Gt/+</sup> mice were obtained under 400 $\times$  magnification from the cortical and medullary region for fibrosis, F4/80, apoptosis, proliferation, and Kim1 levels. ImageJ (v1.51) processing software was used to manually determine threshold values until the regions of interest were highlighted. Identical threshold values were used for all images for fibrosis, F4/80, and Kim1. The percentage of fibrosis, F4/80, and Kim1 staining was calculated relative to the total kidney area of the tissue field. The number of Caspase 3 and Ki-67 cells were counted for renal corpuscles, cortical, and medullary tubules, and divided by total number of cells in each field. Two-tailed *t* test was performed using GraphPad Prism (v8.1.2, USA) to compare levels in WT and Shroom3<sup>Gt/+</sup> mice, *P* values of <0.05 were considered statistically significant, and data are reported as mean  $\pm$  SEM.

### MDCK Cell Culture Experiment

The fluorescent mCherry tag was inserted in frame 5' of the Shroom3 coding sequence in the pCMV-Shroom3-Flag vector as described (15). Then, mCherry-Shroom3 was cloned into the EagI restriction site of the pTre3G plasmid (Takara Bio, USA). Stable MDCK cell lines were generated with the Tet-On inducible expression system (Clontech, USA) using

the pCMV-Tet3G and pTre3G-mCherry-Shroom3 plasmids, and hygromycin/G418 dual selection. Cells were plated on Lumox culture dishes, allowed to reach confluency, treated with doxycycline (1  $\mu\text{g}/\text{ml}$ ) for 24 hours, and fixed with 4% PFA for 1 hour. Cells were then immunolabeled using primary antibodies ( $\alpha$ -Flag, Sigma F3165;  $\alpha$ -non-muscle myosin IIB, #PRB-445P), stained for F-actin (phalloidin-647, Invitrogen) and imaged by fluorescence microscopy. ImageJ was utilized to measure the intensity of >50 random bicellular junctions from three different experiments images using the line tool, and the apical cortex of >50 cells from three different experiments using the ellipse tool.

## Results and Discussion

Shroom3 is a risk gene for CKD (8,9), reduced eGFR (8,9), and post-transplant renal fibrosis (12,28,29), yet its causative mechanisms in kidney disease and kidney repair are unknown. Several of the Shroom3 variants associated with impaired kidney function are predicted to alter the expression levels of Shroom3, alter Shroom3 function, and some variants are predicted to be damaging to protein function (26). To begin to understand the associations of Shroom3 with kidney disease, we initially defined the Shroom3 protein expression in 3-month-old WT kidneys. In WT mice, Shroom3 primarily localized to the apical regions of the cortical tubular epithelium (Figure 1, A and B). To better understand Shroom3's potential pathologic role in kidney disease and repair, we utilized WT and Shroom3 heterozygous null mice (*Shroom3*<sup>Gt/+</sup>) and subjected them to IRI. The *Shroom3*<sup>Gt/+</sup> mutant mice do not exhibit any overt phenotypic alterations when compared with WT littermates (Supplemental Figure 1). Furthermore, both WT and *Shroom3*<sup>Gt/+</sup> mutants exhibited identical Shroom3 protein expression pattern after AKI (IRI), although the Shroom3 protein levels were reduced, as expected in heterozygous mice (Figure 1B). Further, no expression of Shroom3 was observed in cells of the interstitium in WT or *Shroom3*<sup>Gt/+</sup> mutants before or after IRI (Figure 1, A and B and Supplemental Figure 1). We utilized *Shroom3*<sup>Gt/+</sup> heterozygous null mice in this analysis, rather than *Shroom3*<sup>Gt/Gt</sup> homozygous null mice. The *Shroom3*<sup>Gt/Gt</sup> homozygous null mice die at birth due to exencephaly, which prevents any postnatal analysis (23). Taken together, these studies confirm the *Shroom3*<sup>Gt/+</sup> heterozygous null mice are phenotypically similar to WT mice at 3 months, with the exception of exhibiting reduced Shroom3 expression levels.

To investigate the potential pathologic role of Shroom3 in kidney disease and kidney repair, WT and *Shroom3*<sup>Gt/+</sup> mice were subjected to IRI by clamping the renal pedicles bilaterally for 28 minutes. This AKI resulted in all *Shroom3*<sup>Gt/+</sup> mice dying within 24 hours of the procedure ( $n=6$ ). This prevented any further functional and histologic analysis (Figure 1C). This prompted us to perform the IRI procedure for 22 minutes. After 48 hours, WT mice had a mortality rate of 7% (one of 14) and *Shroom3*<sup>Gt/+</sup> mice had 23% (six of 26) (Figure 1D). After 10 days, the mortality rate was 14% (two of 14) in WT mice and 35% (nine of 26) in *Shroom3*<sup>Gt/+</sup> mice (Figure 1D). Although the increased

mortality could be caused by extensive tissue damage to the kidney itself, there could be other contributing factors. AKI can affect other organ systems such as the brain, heart, and lungs. Considering Shroom3 is expressed in each of these organs, it would be interesting to determine if an AKI injury has effects in these organs and whether Shroom3 plays a role.

To better understand the consequences of reduced Shroom3 expression on the kidney, we next analyzed the histopathology at 48 hours after injury. The WT mice demonstrated focal areas of dilated cortical tubules containing small amounts of cellular debris in cortical tubule lumens (Figure 1E). The medullary tubules exhibited no marked alterations (Figure 1I). In contrast, the cortical tubules in *Shroom3*<sup>Gt/+</sup> mice exhibited a substantial number of dilated tubules containing cellular debris and protein casts (Figure 1F). These tubules exhibited epithelial flattening, loss of brush border, and cell detachment (Figure 1F). Almost all of the medullary tubules were also dilated and contained protein casts (Figure 1J). By 10 days, WT kidneys demonstrated little observable tissue damage in the cortex or medulla (Figure 1, G and K). Conversely, *Shroom3*<sup>Gt/+</sup> kidneys at 10 days still exhibited severe cortical and medullary histopathology (Figure 1, H and L). The analysis of the Sham-operated controls in Wild-type or *Shroom3*<sup>Gt/+</sup> kidneys did not exhibit any observable histopathology (Supplemental Figure 2, A–C). This analysis indicates the WT mice progress through the tissue reparative processes after an AKI, but the *Shroom3*<sup>Gt/+</sup> mice do not. We next performed a kidney function analysis after IRI using serum creatinine assay. The WT mice exhibited a two-fold increase in serum creatinine at 24 hours, which returned to baseline after 48 hours (Figure 1M). In contrast, *Shroom3*<sup>Gt/+</sup> mice demonstrated a 3.8-fold increase in serum creatinine at 24 hours when compared with baseline levels (Figure 1M), indicating a more severe effect on kidney function after 24 hours. The levels remained elevated in the *Shroom3*<sup>Gt/+</sup> mice at 48 hours and trended toward baseline levels by 7 days (Figure 1M). This indicates that *Shroom3*<sup>Gt/+</sup> mice do make a full functional recovery, but this recovery is delayed and is associated with poor histopathology.

After an AKI, several cellular and molecular processes are activated to repair the kidney (30). However, if the repair processes are altered or inefficient, this can result in extensive tissue remodeling and renal fibrosis. Our analysis of *Shroom3*<sup>Gt/+</sup> mice after 10 days demonstrated a significant amount of interstitial fibrosis around the renal corpuscles (Figure 2, A and B), proximal tubules (Figure 2, A and B), and collecting ducts (Figure 2, D and E). Quantitative analysis demonstrated a 4.35-fold increase in cortical fibrosis (Figure 2, A–C) and a 5.86-fold increase in the medullary fibrosis when compared with WT (Figure 2, A–C). We were therefore interested in the mechanisms of how *Shroom3*<sup>Gt/+</sup> mice exhibited increased fibrosis. Myofibroblasts are the dominant cells that contribute to the deposition of extracellular matrix and thus leading to fibrosis (30,31). Therefore, we analyzed WT and *Shroom3*<sup>Gt/+</sup> kidneys for  $\alpha$ SMA, a marker of myofibroblasts. In WT,  $\alpha$ SMA was observed in select tubular epithelial cells but was largely absent in the interstitium at both 48 hours and 10 days (Figure 2D). In contrast, widespread  $\alpha$ SMA

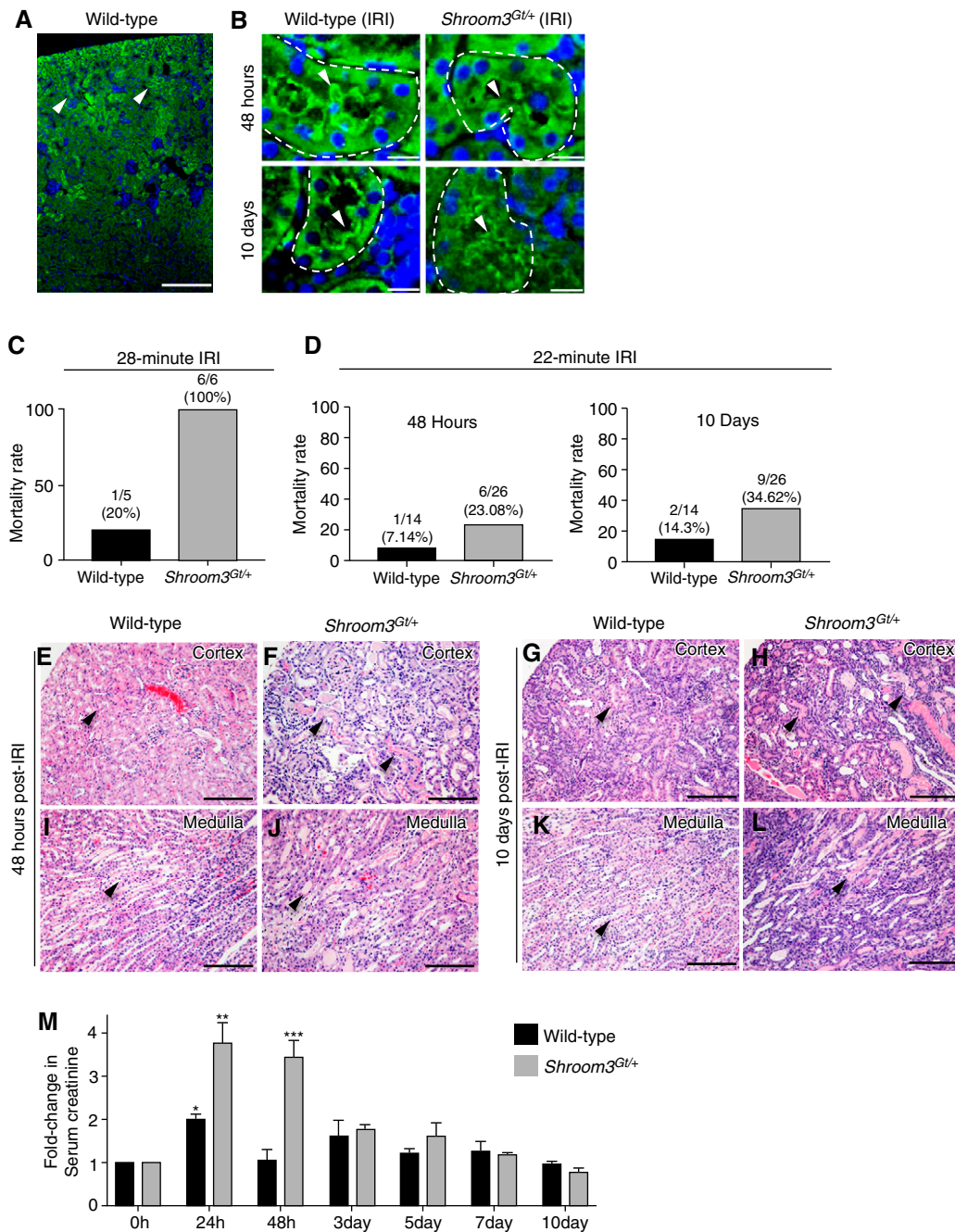


**Figure 1. | *Shroom3<sup>Gt/+</sup>* mice exhibit worse ischemia reperfusion kidney injury (IRI)-induced tubular injury** (A) Immunofluorescence (IF) demonstrating Shroom3 expression primarily in cortical tubular epithelium (arrowhead). (B) Shroom3 expression continues to be expressed in cortical tubules 48 hours and 10 days after IRI (arrowhead). The levels of Shroom3 expression are reduced in *Shroom3<sup>Gt/+</sup>* tubules but the spatial pattern remains identical. (C) and (D) *Shroom3<sup>Gt/+</sup>* mice have higher mortality rates after a 28-minute and 22-minute IRI. (E)–(L) Representative H&E-stained kidney tissue 48 hours and 10 days after IRI. After 48 hours *Shroom3<sup>Gt/+</sup>* kidneys exhibit more severe cortical and medullary tubular damage (arrowheads) when compared with WT (E)–(H). After 10 days the *Shroom3<sup>Gt/+</sup>* kidneys exhibit severe histopathology although the WT mice have recovered (I)–(L). (M) Analysis of kidney function. Wild-type mice show a two-fold increase in serum creatinine levels at 24 hours after IRI,  $P=0.02$  (\*), which returned to baseline levels by 48 hours. In contrast, *Shroom3<sup>Gt/+</sup>* mice show a 3.8-fold increase in serum creatinine levels after 24 hours,  $P<0.0001$  (\*\*), which persisted at 48 hours after IRI,  $P<0.0001$  (\*\*\*) and trended to baseline levels by day 10. Scale bars = 400  $\mu\text{m}$  (A), 10  $\mu\text{m}$  (B), 200  $\mu\text{m}$  (E)–(L). WT = wild-type.

expression was observed primarily in the tubules and interstitium of *Shroom3<sup>Gt/+</sup>* kidneys at 48 hours and 10 days (Figure 2E). This indicated there was an extensive expansion of myofibroblasts and fibrosis in the *Shroom3<sup>Gt/+</sup>*

kidneys in response to the AKI, suggesting a potential mechanism of the worse kidney injury.

There has been some debate as to the origin of the expanding myofibroblast cell population. Studies have

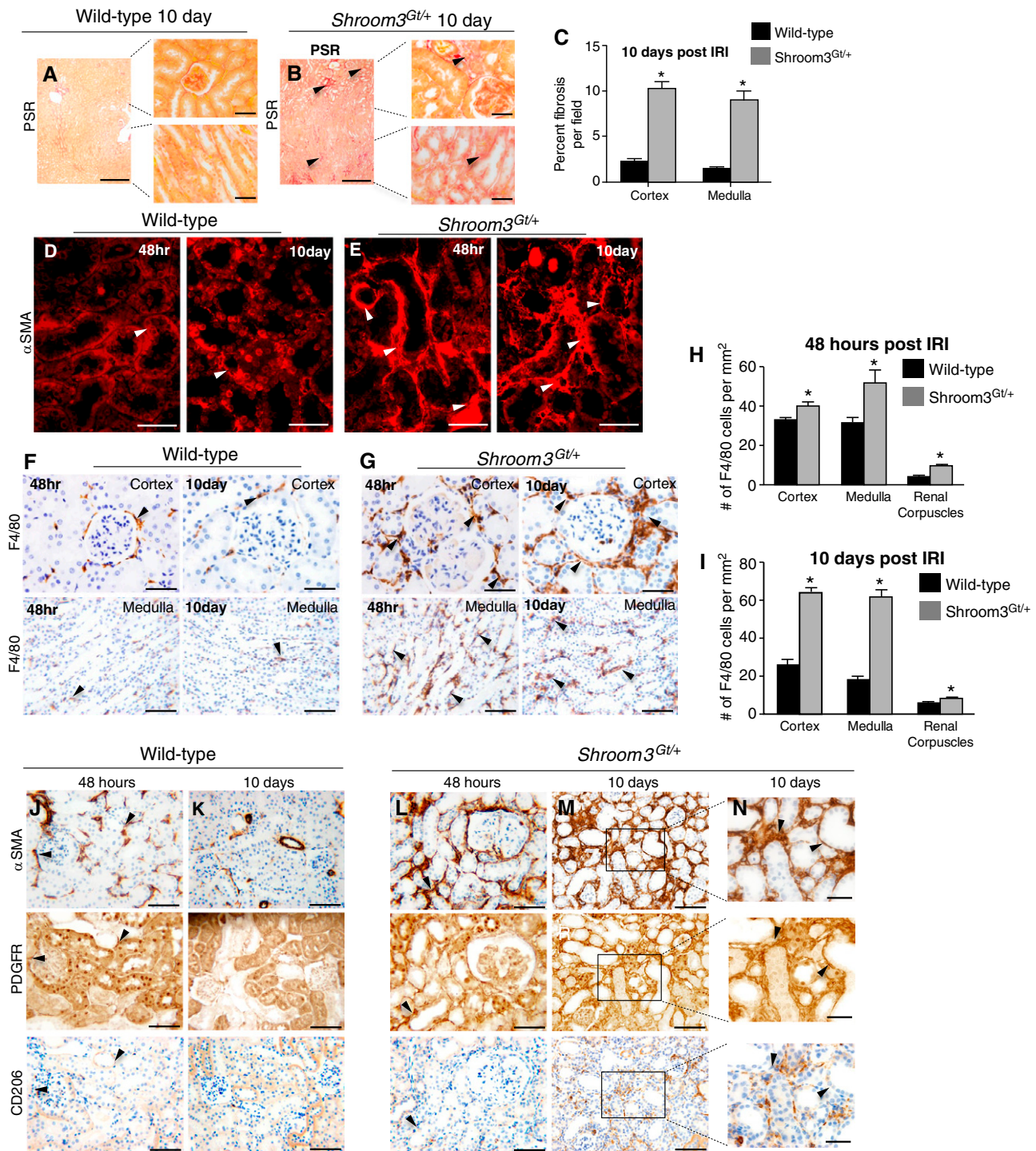


**Figure 2. | *Shroom3<sup>Gt/+</sup>* mice exhibit expanded fibrosis after renal IRI.** (A) (B) Representative low- and high-power picrosirius red-stained kidney tissue from WT and *Shroom3<sup>Gt/+</sup>*. (A)–(C) Qualitative and quantitative analysis demonstrates increased cortical and medullary interstitial fibrosis surrounding cortical and medullary tubules (arrowheads). (D) and (E) IF of  $\alpha$ SMA expression in WT and *Shroom3<sup>Gt/+</sup>* (arrowhead). In contrast to WT (D), *Shroom3<sup>Gt/+</sup>* exhibit an expanded expression at 48 hours and 10 days after IRI in the tubular epithelium and interstitium. (F)–(I) Representative images of F4/80 IHC in cortex and medulla from WT and *Shroom3<sup>Gt/+</sup>* at 48 hours and 10 days after IRI. (H) and (I) Quantitation of F4/80<sup>+</sup> cells demonstrating *Shroom3<sup>Gt/+</sup>* mice exhibit more F4/80<sup>+</sup> cells around the cortex, renal corpuscles, and medulla. (J)–(N) Representative images of serial sections of WT and *Shroom3<sup>Gt/+</sup>* mutants 10 days after IRI and IHC performed for  $\alpha$ SMA, PDGFR $\beta$ , CD206 demonstrating  $\alpha$ SMA cells primarily derive from resident fibroblasts in *Shroom3<sup>Gt/+</sup>* mutants (arrowheads). \* $P < 0.0001$ . Scale bars = 400  $\mu$ m (A) and (B) insets = 40  $\mu$ m, 40  $\mu$ m (D)–(G) and (N), 80  $\mu$ m (J)–(M). WT = wild-type.

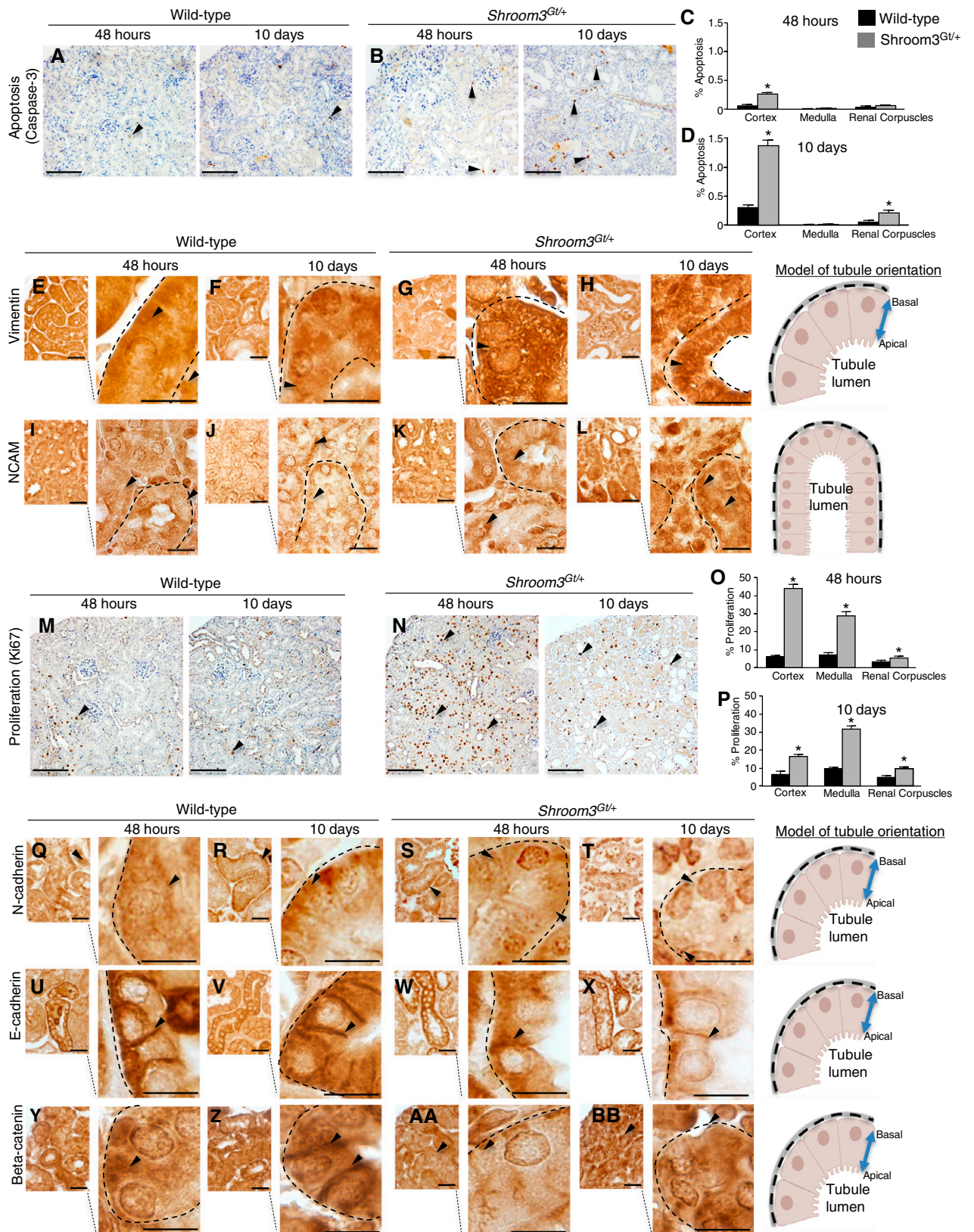


**Figure 3. | *Shroom3<sup>Gt/+</sup>* mice exhibit altered recovery and epithelial differentiation after IRI.** (A) and (B) Representative low- and high-power images demonstrating caspase-3 immunohistochemistry indicating dying cells (arrowheads). (A)–(D) Qualitative and quantitative analysis demonstrates a significant increase in the number of apoptotic cells in the cortex and renal corpuscles in *Shroom3<sup>Gt/+</sup>* mutants 10 days after IRI. (E)–(L) Representative low- and high-power images of IHC for vimentin (E)–(H) and NCAM (I)–(L) in kidney tissue from

suggested it could be due to macrophage transdifferentiation and/or interstitial fibroblast activation (32). Therefore, we next analyzed WT and *Shroom3*<sup>Gt/+</sup> kidneys for F4/80+, a marker of circulating and resident macrophages (33). In WT, scarce F4/80+ cells were found in the interstitium surrounding the nephrons and medullary tubules at 48 hours and the number of these F4/80+ cells was reduced significantly by 10 days (Figure 2, F, H, and I). In contrast, *Shroom3*<sup>Gt/+</sup> mice exhibited a substantial number of F4/80+ cells surrounding the glomeruli and cortical and medullary tubules at 48 hours, and the number of F4/80+ cells increased at 10 days (Figure 2, G, H, and I). This means there is an expansion of the macrophage cell population, but whether the macrophages are resident or infiltrating from the circulation is not known. Therefore, we next performed serial section IHC for  $\alpha$ SMA, CD206, and PDGFR $\beta$ . CD206 is a marker of infiltrating and alternatively activated profibrotic macrophages (34,35), and PDGFR $\beta$  is a marker of resident fibroblasts (36,37). In WT tissue, some  $\alpha$ SMA-positive cells expressed PDGFR $\beta$  (Figure 2, J and K), but no overlapping expression of CD206 was observed at 48 hours or 10 days (Figure 2, J and K). *Shroom3*<sup>Gt/+</sup> mice exhibited overlapping  $\alpha$ SMA and PDGFR $\beta$  expression at 48 hours, however, very little CD206 expression was observed and no overlap was observed (Figure 2L). After 10 days, many of the  $\alpha$ SMA cells overlapped with PDGFR $\beta$ -expressing cells (Figure 2, M and N). However, clusters of CD206-expressing cells exhibited minimal overlap with  $\alpha$ SMA cells (Figure 2, M and N). These data demonstrate the majority of the expanding myofibroblast population in our model system is derived from resident fibroblasts. Our data also support that a small proportion of infiltrating macrophages also contributes to the myofibroblast population. The data that we observed in our model system are consistent with other reports in different model systems (32).

We next analyzed apoptosis using a morphologic and biochemical analysis. The analysis of cell death after 48 hours revealed a modest increase in the cortical and medullary tubules and renal corpuscles in *Shroom3*<sup>Gt/+</sup> kidneys when compared with WT (Figure 3, A–D). However, after 10 days of recovery, *Shroom3*<sup>Gt/+</sup> kidneys exhibited significant levels of apoptosis in the tubular epithelium, culminating in a four-fold increase in cortical apoptosis and a three-fold increase in renal corpuscle apoptosis in *Shroom3*<sup>Gt/+</sup> kidneys (Figure 3, C and D). Programmed cell death after AKI removes the damaged or dying cells usually by shedding them into the tubular lumen (38) or through phagocytosis by neighboring epithelial cells. These data suggest a large number of damaged cells are being removed during the initial stages of re-establishing the functional epithelium (38,39). As the damaged cells are removed, there is an

onset of mesenchymal cell marker expression such as vimentin and NCAM, which indicates epithelial-to-mesenchymal transition (40,41,42). At 48 hours after IRI, vimentin and NCAM expression are observed in the tubular epithelium in both WT and *Shroom3*<sup>Gt/+</sup> kidneys (Figure 3, E, G, I, and K). By 10 days, low levels of vimentin and NCAM are observed in a few tubular epithelial cells in WT mice (Figure 3, F and J). In contrast, the *Shroom3*<sup>Gt/+</sup> kidneys exhibited increased vimentin and NCAM expression in the tubular epithelium and in cells directly adjacent to the tubules (Figure 3, H and L). After dedifferentiation, the injured epithelia begin the repair process through proliferation of the dedifferentiated tubular epithelia to restore the cells lost during the injury. In *Shroom3*<sup>Gt/+</sup> mutants after 48 hours, a seven-fold and four-fold increase in proliferating cells was observed in the cortex and medulla, respectively, when compared with WT (Figure 3, M–P). The proliferating cells can be observed in the tubular epithelium and to a lesser extent in the interstitium and renal corpuscle (Figure 3, M and N). By 10 days, the cortical cell proliferation in *Shroom3*<sup>Gt/+</sup> mutants remained significantly higher when compared with WT (Figure 3, M and N). Altogether the continued apoptosis, dedifferentiation, and cell proliferation is consistent with the inability to recover after the IRI AKI (43).

Essential to tubular repair is that dedifferentiated epithelial cells re-establish epithelial markers, such as E-cadherin and N-cadherin (3). In both WT and *Shroom3*<sup>Gt/+</sup> mutants after 48 hours of recovery, N-cadherin, primarily a marker of the proximal tubule, was mostly cytoplasmic (Figure 3, Q and S). By 10 days, WT kidneys re-established N-cadherin in the basolateral membrane of the cortical tubules, but the *Shroom3*<sup>Gt/+</sup> mutants did not recover this basolateral expression (Figure 3, R and T). This indicates the proximal tubules in *Shroom3*<sup>Gt/+</sup> mutants are not able to recover the normal epithelial protein expression pattern. At both 48 hours and 10 days, tubular E-cadherin, a primary marker of the distal convoluted tubule, localized between cell to cell junctions and in basolateral membranes in tubular epithelial cells in WT (Figure 3, U and V). In *Shroom3*<sup>Gt/+</sup> mutants at 48 hours, E-cadherin was also observed in the basolateral membranes, although this appeared to be at lower levels in cell to cell junctions (Figure 3, W and X). Although this indicates both major cortical tubules are affected, the reduced expression of Shroom3 affects the proximal tubule more severely. The stabilization of adherens junctions is also essential for re-establishing the tubular epithelium (44). The analysis of beta-catenin, a key adherens junction protein, confirmed the disrupted tubular epithelium and poorly established junctions in *Shroom3*<sup>Gt/+</sup> mutant tubular epithelium (Figure 3, Y–BB). Altogether, these data demonstrate that after IRI, WT

**Figure 3.** | Continued. WT and *Shroom3*<sup>Gt/+</sup>. In contrast to WT, *Shroom3*<sup>Gt/+</sup> mutants exhibit increased expression of Vimentin and NCAM after 10 days of IRI (arrowheads). (M) and (N) Representative low- and high-power images of Ki67 IHC in WT and *Shroom3*<sup>Gt/+</sup> mutants 48 hours and 10 days after IRI indicating cell proliferation (arrowheads). (O) and (P) Qualitative and quantitative analysis demonstrates significant increases in the number of proliferating cells in *Shroom3*<sup>Gt/+</sup> mutants 48 hours and 10 days after IRI. (Q)–(BB) Representative low- and high-power images of IHC for N-cadherin (Q)–(T), E-cadherin (U)–(X), and beta-catenin (Y)–(BB) in kidney tissue from WT and *Shroom3*<sup>Gt/+</sup>. Wild-type kidneys re-establish the tubular epithelial junctional proteins 10 days after IRI, which is not observed in the *Shroom3*<sup>Gt/+</sup> mutants (arrowheads). \**P*≤0.0001. Scale bars = 200  $\mu$ m (A), (B), (M), and (N), 40  $\mu$ m (E)–(L), insets = 10  $\mu$ m, 20  $\mu$ m (Q)–(BB) insets = 10  $\mu$ m. WT = wild-type.

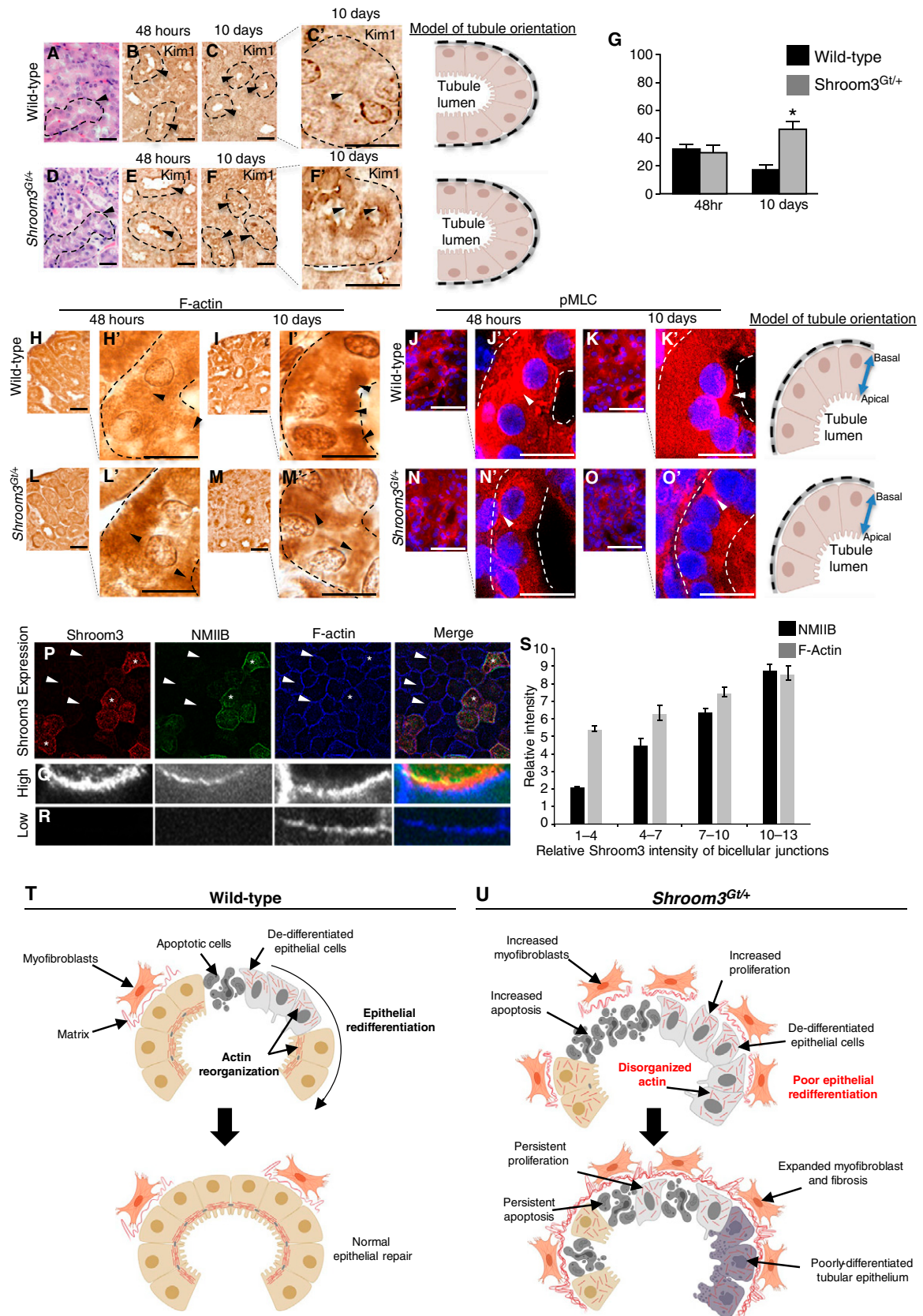


**Figure 4. | Actomyosin signaling during epithelial kidney repair is Shroom3 dependent.** (A)–(F) Representative images of H&E demonstrating altered tubular epithelial morphology, (A) and (D) dotted line and arrowheads, and persistent tubular epithelial injury by Kim1 IHC expression (B), (C), (E), and (F) dotted line and arrowheads, 10 days after IRI injury. (G) Quantitative analysis demonstrating Kim1



and *Shroom3*<sup>Gt/+</sup> epithelial cells are capable of dedifferentiating and expressing mesenchymal markers, demonstrating that reduced Shroom3 levels do not disrupt this process. However, the *Shroom3*<sup>Gt/+</sup> dedifferentiated epithelial cells continue to express mesenchymal markers, and therefore these data support a role for Shroom3 in epithelial repair by affecting the epithelial redifferentiation.

Although the kidney function in *Shroom3*<sup>Gt/+</sup> mice fully recovers, H&E analysis demonstrates significant histopathology characterized by marked tubular damage, indicating a lack of tubular repair (Figure 4, A and D). To confirm the kidneys still exhibit kidney injury, we analyzed tissue for Kim1, a protein that is expressed in injured tubules (45). In WT cells, Kim1 was upregulated in the apical border of the tubular epithelium at 48 hours and its protein expression was nearly absent by 10 days (Figure 4, B, C, and G). In *Shroom3*<sup>Gt/+</sup> mutants, Kim1 protein expression was also upregulated after 48 hours (Figure 4E). However, at 10 days Kim1 expression continued to be expressed at high levels in the apical border of *Shroom3*<sup>Gt/+</sup> mutants (Figure 4, F and G). These data support that the *Shroom3*<sup>Gt/+</sup> mutants continue to exhibit injury and therefore the mechanisms of tubular repair could be altered. Actin cytoskeleton organization and reassembly is essential for re-establishing epithelial polarity during epithelial repair (27). Further, Shroom3 modulates the actin intracellular distribution by recruiting and binding actin to the apical region of cells (18). The analysis of F-actin demonstrated it was distributed in a cytoplasmic pattern in both WT (Figure 4H) and *Shroom3*<sup>Gt/+</sup> mutants (Figure 4L) in the tubular epithelium at 48 hours. After 10 days, WT kidneys exhibited strong apical localization of F-actin in majority of the tubular epithelium, indicating actin was redistributed to the apical portion of the cell (Figure 4I). However, the tubular epithelium in *Shroom3*<sup>Gt/+</sup> mutant kidneys clearly lacked the apical expression pattern (Figure 4M). Instead, the *Shroom3*<sup>Gt/+</sup> mutants exhibited a more basolateral and intracellular pattern, suggesting defects in its redistribution to the apical region of the cells (Figure 4M). We next analyzed phosphorylation of myosin light chain (pMLC), which is a downstream effector in the Shroom3/ROCK signaling pathway and is necessary for cell contractility (17,46). In WT kidneys after 48 hours, pMLC was absent from the apical portion of the cell, but the apical expression returned by 10 days in the tubular epithelium (Figure 4, J and K). As expected, pMLC in *Shroom3*<sup>Gt/+</sup> mutants was not apically observed at 48 hours (Figure 4N). However, at 10 days pMLC remained absent in the apical region of the cell in *Shroom3*<sup>Gt/+</sup> mutants and instead remained in the basolateral aspect of the cell (Figure 4O). The transition to an

epithelial morphology and integration into the tubule is dependent on proper actomyosin organization and contractility. Our *in vivo* results suggest reduced Shroom3 expression disrupts the actin localization to the apical membrane after an IRI, thereby disrupting the proper regulation of the actomyosin dynamics.

We next confirmed the mislocalization of F-actin and pMLC in the tubular epithelium in *Shroom3*<sup>Gt/+</sup> mutants using MDCK cells, which are isolated kidney tubular cells that naturally express low levels of Shroom3 (15). MDCK cells stably transfected with Shroom3 demonstrate variable amounts of Shroom3 expression (Figure 4P, asterisks for high expressing, arrowheads for low expressing). In the higher Shroom3-expressing cells, the costaining for Shroom3, nonmuscle myosin IIB, and F-actin revealed immunofluorescence of all three proteins was robustly apically colocalized at bicellular junctions (Figure 4, P and Q). However, in low Shroom3-expressing MDCK cells (Figure 4P, arrowheads) the reduced expression of Shroom3 was consistently associated with reduced nonmuscle myosin IIB and F-actin in the apical region of the cells (Figure 4, P and R). We next quantitated the average pixel density of muscle myosin IIB/and F-actin immunolabeled MDCK cells expressing variable amounts of Shroom3. In low-expressing Shroom3 cells, the expression of nonmuscle myosin IIB and F-actin were consistently reduced when compared with the higher expressing Shroom3 MDCK cells (Figure 4S). These *in vitro* results support our *in vivo* data that show Shroom3 regulates proper tubular epithelial repair through the regulation of actomyosin organization.

In the search for new genes associated with kidney disease, genome-wide association studies have identified numerous genetic variants in *SHROOM3* that are associated with kidney function and kidney disease. Despite these strong and numerous association studies, the Shroom3 functions and the mechanistic understanding behind these associations remain a knowledge gap in molecular nephrology. Taken together, the absence of the correct dose and function of Shroom3 results in worse tubular epithelial damage, leading to increased apoptosis, proliferation, inflammatory cell infiltration, and expanded myofibroblast activity leading to fibrosis (Figure 4, T and U). Further, the lack of proper actin and actomyosin regulation and organization results in a reduced reestablishment of epithelial markers, indicative of altered epithelial redifferentiation resulting in continued tubular epithelial damage and remodeling. On the basis of the incomplete repair of the kidney tissue, it is likely additional kidney challenges could progress to CKD (Figure 4, T and U). Further, the tubular epithelial cells are constantly undergoing repair

**Figure 4.** | Continued. expression in the cortical tubular epithelium in WT and *Shroom3*<sup>Gt/+</sup> mutants 10 days after IRI. (H)–(O) Representative low- and high-power images of immunostaining for F-actin and phosphorylation of myosin light chain (pMLC) in WT and *Shroom3*<sup>Gt/+</sup> mutants 48 hours and 10 days after IRI. Then 10 days after kidney injury, F-actin and pMLC protein expression is apically localized in WT tubular epithelium but not in *Shroom3*<sup>Gt/+</sup> mutants (dotted line and arrowheads). (P)–(R) Representative low- (P) and high-power (Q), (R) images of the MDCK apical cell membrane after immunolabeling for Shroom3, nonmuscle myosin IIB (NMIIB), and F-actin. (Q) High expressing Shroom3 cells exhibit robust immunofluorescent signal in the apical membrane (\*). (R) Low-expressing Shroom3 cells exhibit a reduced apical NMIIB and F-actin expression (arrowheads). (S) Quantitation of pixel density of MDCK cells immunolabeled for Shroom3, NMIIB, and F-actin. Low-expressing Shroom3 cells express lower levels of NMIIB and F-actin compared with the higher expressing Shroom3 MDCK cells. \**P* ≤ 0.0001. Scale bars = 40 μm (A)–(O), insets = 10 μm. WT = wild-type.

and regeneration under normal physiologic conditions (47). Therefore, disruptions in *Shroom3* expression or function could lead to incomplete epithelial repair, which may also culminate in CKD. Altogether, we provided novel experimental evidence into the molecular mechanisms of cortical tubular repair post-AKI and identified *Shroom3* as an important player. Further, these studies could also provide key mechanistic insight to explain why genetic variants in *Shroom3* are strongly associated with allograft rejection and CKD. Our hope is that this fundamental knowledge will provide improved risk stratification and the generation of novel therapeutic strategies.

#### Disclosures

K. Ask reports receiving grants from Alkermes, Bold Therapeutics, Canadian Institute for Health Research, Canadian Pulmonary Fibrosis Association, Ceapro, Collaborative Health Research Projects, CSL Behring, GSK, Indalo, Pharmaxis, Pieris Pharmaceuticals, Pliant, Prometic, and Unity Biotechnology, and grants and personal fees from Boehringer Ingelheim, outside of the submitted work. All remaining authors have nothing to disclose.

#### Funding

This work was supported by the Gouvernement du Canada, Canadian Institute of Health Research (142264), Institute of Nutrition, Metabolism and Diabetes, McMaster University (2-15105); Gouvernement du Canada, National Sciences and Engineering Research Council of Canada (RGPIN 2021-04289), and the Kidney Foundation of Canada (856593-21KHRG).

#### Author Contributions

D. Bridgewater conceptualized the study; K. Ask, D. Bridgewater, J. Cunanan, A. Hunjan, H. Khalili, A. Khan, A. Li, and T. Plageman were responsible for the data curation; D. Bridgewater, J. Cunanan, H. Khalili, and A. Li were responsible for the formal analysis; D. Bridgewater was responsible for the funding acquisition; D. Bridgewater, J. Cunanan, and A. Li were responsible for the investigation; D. Bridgewater, J. Cunanan, H. Khalili, A. Li, and T. Plageman were responsible for the methodology; D. Bridgewater was responsible for the project administration; K. Ask and T. Drysdale were responsible for the resources; D. Bridgewater was responsible for the software; D. Bridgewater and J. Cunanan provided supervision; D. Bridgewater and H. Khalili were responsible for the validation; D. Bridgewater was responsible for the visualization; and D. Bridgewater and J. Cunanan wrote the original draft and reviewed and edited the manuscript.

#### Supplemental Material

This article contains the following supplemental material online at <http://kidney360.asnjournals.org/lookup/suppl/doi:10.34067/KID.0003802021/-/DCSupplemental>.

Supplemental Figure 1. Representative low- and high-power images of H&E-stained wild-type (WT) and *Shroom3*<sup>Gt/+</sup> mutants at 3 months of age.

Supplemental Figure 2. Representative low- and high-power images of Sham-operated wild-type (WT) and *Shroom3*<sup>Gt/+</sup> mice 48 hours post-IRI.

#### References

- Bonventre JV, Yang L: Cellular pathophysiology of ischemic acute kidney injury. *J Clin Invest* 121: 4210–4221, 2011 <https://doi.org/10.1172/JCI45161>
- Bridgewater D, Cox B, Cain J, Lau A, Athaide V, Gill PS, Kuure S, Sainio K, Rosenblum ND: Canonical WNT/beta-catenin signaling is required for ureteric branching. *Dev Biol* 317: 83–94, 2008 <https://doi.org/10.1016/j.ydbio.2008.02.010>
- Thiery JP, Sleeman JP: Complex networks orchestrate epithelial-mesenchymal transitions. *Nat Rev Mol Cell Biol* 7: 131–142, 2006 <https://doi.org/10.1038/nrm1835>
- Bonventre JV: Dedifferentiation and proliferation of surviving epithelial cells in acute renal failure. *J Am Soc Nephrol* 14[Suppl 1]: S55–S61, 2003 <https://doi.org/10.1097/01.ASN.0000067652.51441.21>
- Coca SG, Singanamala S, Parikh CR: Chronic kidney disease after acute kidney injury: A systematic review and meta-analysis. *Kidney Int* 81: 442–448, 2012 <https://doi.org/10.1038/ki.2011.379>
- Chawla LS, Kimmel PL: Acute kidney injury and chronic kidney disease: An integrated clinical syndrome. *Kidney Int* 82: 516–524, 2012 <https://doi.org/10.1038/ki.2012.208>
- Grandaliano G, Castellano G, Gesualdo L: Maladaptive repair and progression to CKD. In: *Critical Care Nephrology, 3rd Ed., Amsterdam, Elsevier*, 2019, pp 159–163
- Köttgen A, Glazer NL, Dehghan A, Hwang SJ, Katz R, Li M, Yang Q, Gudnason V, Launer LJ, Harris TB, Smith AV, Arking DE, Astor BC, Boerwinkle E, Ehret GB, Ruczinski I, Scharpf RB, Chen YD, de Boer IH, Haritunians T, Lumley T, Sarnak M, Siscovick D, Benjamin EJ, Levy D, Upadhyay A, Aulchenko YS, Hofman A, Rivadeneira F, Uitterlinden AG, van Duijn CM, Chasman DI, Paré G, Ridker PM, Kao WH, Witteman JC, Coresh J, Shlipak MG, Fox CS: Multiple loci associated with indices of renal function and chronic kidney disease. *Nat Genet* 41: 712–717, 2009 <https://doi.org/10.1038/ng.377>
- Böger CA, Gorski M, Li M, Hoffmann MM, Huang C, Yang Q, Teumer A, Krane V, O’Seaghdha CM, Kutalik Z, Wichmann HE, Haak T, Boes E, Coassin S, Coresh J, Kollerits B, Haun M, Paulweber B, Köttgen A, Li G, Shlipak MG, Powe N, Hwang SJ, Dehghan A, Rivadeneira F, Uitterlinden A, Hofman A, Beckmann JS, Krämer BK, Witteman J, Bochud M, Siscovick D, Rettig R, Kronenberg F, Wanner C, Thadhani RI, Heid IM, Fox CS, Kao WH; CKDGen Consortium: Association of eGFR-related loci identified by GWAS with incident CKD and ESRD. *PLoS Genet* 7: e1002292, 2011 <https://doi.org/10.1371/journal.pgen.1002292>
- Böger CA, Heid IM: Chronic kidney disease: Novel insights from genome-wide association studies. *Kidney Blood Press Res* 34: 225–234, 2011 <https://doi.org/10.1159/000326901>
- Meyer TE, Verwoert GC, Hwang SJ, Glazer NL, Smith AV, van Rooij FJ, Ehret GB, Boerwinkle E, Felix JF, Leak TS, Harris TB, Yang Q, Dehghan A, Aspelund T, Katz R, Homuth G, Kocher T, Rettig R, Ried JS, Gieger C, Prucha H, Pfeuffer A, Meitinger T, Coresh J, Hofman A, Sarnak MJ, Chen YD, Uitterlinden AG, Chakravarti A, Psaty BM, van Duijn CM, Kao WH, Witteman JC, Gudnason V, Siscovick DS, Fox CS, Köttgen A; Genetic Factors for Osteoporosis Consortium Meta Analysis of Glucose and Insulin Related Traits Consortium: Genome-wide association studies of serum magnesium, potassium, and sodium concentrations identify six loci influencing serum magnesium levels. *PLoS Genet* 6: e1001045, 2010 <https://doi.org/10.1371/journal.pgen.1001045>
- Menon MC, Chuang PY, Li Z, Wei C, Zhang W, Luan Y, Yi Z, Xiong H, Woytovich C, Greene I, Overbey J, Rosales I, Bagiella E, Chen R, Ma M, Li L, Ding W, Djamali A, Saminiego M, O’Connell PJ, Gallon L, Colvin R, Schroppel B, He JC, Murphy B: Intronic locus determines SHROOM3 expression and potentiates renal allograft fibrosis. *J Clin Invest* 125: 208–221, 2015 <https://doi.org/10.1172/JCI76902>
- Lee C, Le MP, Wallingford JB: The shroom family proteins play broad roles in the morphogenesis of thickened epithelial sheets. *Dev Dyn* 238: 1480–1491, 2009 <https://doi.org/10.1002/dvdy.21942>

14. Hagens O, Ballabio A, Kalscheuer V, Kraehenbuhl JP, Schiaffino MV, Smith P, Staub O, Hildebrand J, Wallingford JB: A new standard nomenclature for proteins related to Apx and Shroom. *BMC Cell Biol* 7: 18, 2006 <https://doi.org/10.1186/1471-2121-7-18>
15. Plageman TF Jr, Chung MI, Lou M, Smith AN, Hildebrand JD, Wallingford JB, Lang RA: Pax6-dependent Shroom3 expression regulates apical constriction during lens placode invagination. *Development* 137: 405–415, 2010 <https://doi.org/10.1242/dev.045369>
16. Nishimura T, Takeichi M: Shroom3-mediated recruitment of Rho kinases to the apical cell junctions regulates epithelial and neuroepithelial planar remodeling. *Development* 135: 1493–1502, 2008 <https://doi.org/10.1242/dev.019646>
17. Das D, Zalewski JK, Mohan S, Plageman TF, VanDemark AP, Hildebrand JD: The interaction between Shroom3 and Rho-kinase is required for neural tube morphogenesis in mice. *Biol Open* 3: 850–860, 2014 <https://doi.org/10.1242/bio.20147450>
18. Plageman TF Jr, Chauhan BK, Yang C, Jaudon F, Shang X, Zheng Y, Lou M, Debant A, Hildebrand JD, Lang RA: A Trio-RhoA-Shroom3 pathway is required for apical constriction and epithelial invagination. *Development* 138: 5177–5188, 2011 <https://doi.org/10.1242/dev.067868>
19. Plageman TF Jr, Zacharias AL, Gage PJ, Lang RA: Shroom3 and a Pitx2-N-cadherin pathway function cooperatively to generate asymmetric cell shape changes during gut morphogenesis. *Dev Biol* 357: 227–234, 2011 <https://doi.org/10.1016/j.ydbio.2011.06.027>
20. Loebel DA, Plageman TF Jr, Tang TL, Jones VJ, Muccioli M, Tam PP: Thyroid bud morphogenesis requires CDC42- and SHROOM3-dependent apical constriction. *Biol Open* 5: 130–139, 2016 <https://doi.org/10.1242/bio.014415>
21. Durbin MD, O’Kane J, Lorentz S, Firulli AB, Ware SM: SHROOM3 is downstream of the planar cell polarity pathway and loss-of-function results in congenital heart defects. *Dev Biol* 464: 124–136, 2020 <https://doi.org/10.1016/j.ydbio.2020.05.013>
22. Khalili H, Sull A, Sarin S, Boivin FJ, Halabi R, Svajcer B, Li A, Cui VW, Drysdale T, Bridgewater D: Developmental origins for kidney disease due to Shroom3 deficiency. *J Am Soc Nephrol* 27: 2965–2973, 2016 <https://doi.org/10.1681/ASN.2015060621>
23. Hildebrand JD, Soriano P: Shroom, a PDZ domain-containing actin-binding protein, is required for neural tube morphogenesis in mice. *Cell* 99: 485–497, 1999 [https://doi.org/10.1016/S0092-8674\(00\)81537-8](https://doi.org/10.1016/S0092-8674(00)81537-8)
24. Yeo NC, O’Meara CC, Bonomo JA, Veth KN, Tomar R, Flister MJ, Drummond IA, Bowden DW, Freedman BI, Lazar J, Link BA, Jacob HJ: Shroom3 contributes to the maintenance of the glomerular filtration barrier integrity. *Genome Res* 25: 57–65, 2015 <https://doi.org/10.1101/gr.182881.114>
25. Matsuura R, Hiraishi A, Holzman LB, Hanayama H, Harano K, Nakamura E, Hamasaki Y, Doi K, Nangaku M, Noiri E: SHROOM3, the gene associated with chronic kidney disease, affects the podocyte structure. *Sci Rep* 10: 21103, 2020 <https://doi.org/10.1038/s41598-020-77952-9>
26. Prokop JW, Yeo NC, Ottmann C, Chhetri SB, Florus KL, Ross EJ, Sosonkina N, Link BA, Freedman BI, Coppola CJ, McDermott-Roe C, Leysen S, Milroy LG, Meijer FA, Geurts AM, Rauscher FJ 3rd, Ramaker R, Flister MJ, Jacob HJ, Mendenhall EM, Lazar J: Characterization of coding/noncoding variants for SHROOM3 in patients with CKD. *J Am Soc Nephrol* 29: 1525–1535, 2018 <https://doi.org/10.1681/ASN.2017080856>
27. Sutton TA, Molitoris BA: Mechanisms of cellular injury in ischemic acute renal failure. *Semin Nephrol* 18: 490–497, 1998
28. Yan L, Li Y, Tang JT, An YF, Luo LM, Dai B, Shi YY, Wang LL: The influence of living donor SHROOM3 and ABCB1 genetic variants on renal function after kidney transplantation. *Pharmacogenet Genomics* 27: 19–26, 2017 <https://doi.org/10.1097/FPC.0000000000000251>
29. Wei C, Banu K, Garzon F, Basgen JM, Philippe N, Yi Z, Liu R, Choudhuri J, Fribourg M, Liu T, Cumpelik A, Wong J, Khan M, Das B, Keung K, Salem F, Campbell KN, Kaufman L, Cravedi P, Zhang W, O’Connell PJ, He JC, Murphy B, Menon MC: SHROOM3-FYN interaction regulates nephrin phosphorylation and affects albuminuria in allografts. *J Am Soc Nephrol* 29: 2641–2657, 2018
30. Kumar S: Cellular and molecular pathways of renal repair after acute kidney injury. *Kidney Int* 93: 27–40, 2018 <https://doi.org/10.1016/j.kint.2017.07.030>
31. Meran S, Steadman R: Fibroblasts and myofibroblasts in renal fibrosis. *Int J Exp Pathol* 92: 158–167, 2011 <https://doi.org/10.1111/j.1365-2613.2011.00764.x>
32. LeBleu VS, Taduri G, O’Connell J, Teng Y, Cooke VG, Woda C, Sugimoto H, Kalluri R: Origin and function of myofibroblasts in kidney fibrosis. *Nat Med* 19: 1047–1053, 2013 <https://doi.org/10.1038/nm.3218>
33. Lever JM, Hull TD, Boddu R, Pepin ME, Black LM, Adedoyin OO, Yang Z, Traylor AM, Jiang Y, Li Z, Peabody JE, Eckenrode HE, Crossman DK, Crowley MR, Bolisetty S, Zimmerman KA, Wende AR, Mrug M, Yoder BK, Agarwal A, George JF: Resident macrophages reprogram toward a developmental state after acute kidney injury. *JCI Insight* 4: 125503, 2019 <https://doi.org/10.1172/jci.insight.125503>
34. Li J, Liu CH, Xu DL, Gao B: Clinicopathological significance of CD206-positive macrophages in patients with acute tubulointerstitial disease. *Int J Clin Exp Pathol* 8: 11386–11392, 2015
35. Kim MG, Kim SC, Ko YS, Lee HY, Jo SK, Cho W: The role of M2 macrophages in the progression of chronic kidney disease following acute kidney injury. *PLoS One* 10: e0143961, 2015 <https://doi.org/10.1371/journal.pone.0143961>
36. Higashi AY, Aronow BJ, Dressler GK: Expression profiling of fibroblasts in chronic and acute disease models reveals novel pathways in kidney fibrosis. *J Am Soc Nephrol* 30: 80–94, 2019 <https://doi.org/10.1681/ASN.2018060644>
37. Nakamura J, Sato Y, Kitai Y, Wajima S, Yamamoto S, Oguchi A, Yamada R, Kaneko K, Kondo M, Uchino E, Tsuchida J, Hirano K, Sharma K, Kohno K, Yanagita M: Myofibroblasts acquire retinoic acid-producing ability during fibroblast-to-myofibroblast transition following kidney injury. *Kidney Int* 95: 526–539, 2019 <https://doi.org/10.1016/j.kint.2018.10.017>
38. Havasi A, Borkan SC: Apoptosis and acute kidney injury. *Kidney Int* 80: 29–40, 2011 <https://doi.org/10.1038/ki.2011.120>
39. Ichimura T, Asseldonk EJ, Humphreys BD, Gunaratnam L, Duffield JS, Bonventre JV: Kidney injury molecule-1 is a phosphatidyserine receptor that confers a phagocytic phenotype on epithelial cells. *J Clin Invest* 118: 1657–1668, 2008 <https://doi.org/10.1172/JCI34487>
40. Wang Z, Divanyan A, Jourdeuil FL, Goldman RD, Ridge KM, Jourdeuil D, Lopez-Soler RI: Vimentin expression is required for the development of EMT-related renal fibrosis following unilateral ureteral obstruction in mice. *Am J Physiol Renal Physiol* 315: F769–F780, 2018 <https://doi.org/10.1152/ajprenal.00340.2017>
41. Cunanan J, Deacon E, Cunanan K, Yang Z, Ask A, Morikawa L, Todorova E, Bridgewater D: Quercetin treatment reduces the severity of renal dysplasia in a beta-catenin dependent manner. *PLoS One* 15: e0234375, 2020 <https://doi.org/10.1371/journal.pone.0234375>
42. Lackie PM, Zuber C, Roth J: Polysialic acid and N-CAM localisation in embryonic rat kidney: Mesenchymal and epithelial elements show different patterns of expression. *Development* 110: 933–947, 1990 <https://doi.org/10.1242/dev.110.3.933>
43. Mao H, Li Z, Zhou Y, Li Z, Zhuang S, An X, Zhang B, Chen W, Nie J, Wang Z, Borkan SC, Wang Y, Yu X: HSP72 attenuates renal tubular cell apoptosis and interstitial fibrosis in obstructive nephropathy. *Am J Physiol Renal Physiol* 295: F202–F214, 2008 <https://doi.org/10.1152/ajprenal.00468.2007>
44. Zhou D, Li Y, Lin L, Zhou L, Igarashi P, Liu Y: Tubule-specific ablation of endogenous  $\beta$ -catenin aggravates acute kidney injury in mice. *Kidney Int* 82: 537–547, 2012 <https://doi.org/10.1038/ki.2012.173>
45. Ichimura T, Bonventre JV, Bailly V, Wei H, Hession CA, Cate RL, Sanicola M: Kidney injury molecule-1 (KIM-1), a putative epithelial cell adhesion molecule containing a novel immunoglobulin domain, is up-regulated in renal cells after injury. *J Biol Chem* 273: 4135–4142, 1998 <https://doi.org/10.1074/jbc.273.7.4135>

46. Miller CJ, Harris D, Weaver R, Ermentrout GB, Davidson LA: Emergent mechanics of actomyosin drive punctuated contractions and shape network morphology in the cell cortex. *PLoS Comput Biol* 14: e1006344, 2018 <https://doi.org/10.1371/journal.pcbi.1006344>
47. Schiessl IM, Grill A, Fremter K, Steppan D, Hellmuth MK, Castrop H: Renal interstitial platelet-derived growth factor receptor- $\beta$  cells support proximal tubular regeneration. *J Am Soc Nephrol* 29: 1383–1396, 2018 <https://doi.org/10.1681/ASN.2017101069>
48. Wei Q, Dong Z: Mouse model of ischemic acute kidney injury: Technical notes and tricks. *Am J Physiol Renal Physiol* 303: F1487–F1494, 2012 <https://doi.org/10.1152/ajprenal.00352.2012>

**Received:** June 8, 2021 **Accepted:** October 28, 2021

A.L., J.C., and H.K. equally to this work.